



ORIGINAL ARTICLE

Paeoniflorin improves cognitive dysfunction, restores glutamate receptors, attenuates gliosis and maintains synaptic plasticity in cadmium-intoxicated mice



Jia-Ying Yang^a, Jun Wang^a, Yang Hu^a, Dan-Yang Shen^a, Guan-Li Xiao^b,
Xiao-Yan Qin^{a,*}, Rongfeng Lan^{b,*}

^a Key Laboratory of Ecology and Environment in Minority Areas National Ethnic Affairs Commission, Center on Translational Neuroscience, College of Life and Environmental Sciences, Minzu University of China, Beijing 100081, China

^b School of Pharmaceutical Sciences, Shenzhen University Health Science Center, Shenzhen 518060, China

Received 9 August 2022; accepted 6 November 2022

Available online 11 November 2022

KEYWORDS

GFAP;
IBA1;
PSD95;
Paeoniflorin;
CD68;
Synaptophysin

Abstract Toxic metals exposed to the environment in industrial and agricultural production, such as cadmium (Cd), Plumbum (Pb) and aluminium (Al), are neurotoxic and harmful to brain functions such as learning and memory, and may contribute to neurological disease. In this study, we investigated the neuronal protective effects of Paeoniflorin (PF) in a mouse model of Cd poisoning that showed cognitive dysfunction. PF attenuated Cd-induced multi-organ damage and brain neurotoxicity, consistent with improved behavioral performances in mice. At the molecular level, Cd-induced toxicity attenuated the phosphorylation of glutamate receptors NMDAR2A, NMDAR2B, and GluR2, but increased the phosphorylation of GluR1. In addition, gliosis after Cd toxicity showed an increase in the number of IBA1 or GFAP-positive cells, which contrasted with the loss of neurons and synapses. However, PF treatment alleviated gliosis and maintained glutamate receptor and neuronal activity, as evidenced by the recovery of marker proteins MAP2, PSD95 and synaptophysin. Also, Cd-induced upregulation of CD68, a lysosomal protein that scavenges damaged cellular components in active microglia, was also restored by PF. In conclusion, PF is a potential neuroprotective natural product.

© 2022 The Author(s). Published by Elsevier B.V. on behalf of King Saud University. This is an open access article under the CC BY-NC-ND license (<http://creativecommons.org/licenses/by-nc-nd/4.0/>).

* Corresponding authors.

E-mail addresses: bjqinxiaoyan@muc.edu.cn (X.-Y. Qin), lan@szu.edu.cn (R. Lan).

Peer review under responsibility of King Saud University.



1. Introduction

Abnormal deposition of toxic metals such as Cd, Pb and Al in the center of senile plaques formed by amyloid- β has been observed (Chin-Chan et al., 2015). In particular, Cd can be enriched in the organism through occupational exposure to industrial and domestic pollution, such as food contamination and smoking, leading to acute or chronic Cd toxicity in the liver, kidneys, reproductive system and brain (Li et al., 2012, Peng et al., 2017). Cd penetrates the blood–brain barrier (BBB) and induces oxidative stress, inflammation and subsequent neuronal death in the central nervous system (CNS), which may lead to vulnerability to neurological disorders such as Alzheimer's disease (AD), Parkinson's disease (PD), depression and schizophrenia (Han et al., 2016, Gustin et al., 2018, Shu et al., 2022). In addition, Cd directly causes damages to the choroid plexus, which is an important structure of the BBB, leading to its destruction (Valois and Webster 1989). Although the pathogenesis of AD is multifaceted, environmental hazards may be one of the important susceptibility factors.

Natural active ingredients are a promising source for exploring compounds for the therapy of neurodegenerative diseases. In previous studies, we established that photoactive chemicals such as THSG (2,3,5,4'-tetrahydroxystilbene-2-O- β -D-glucoside), CE (*Coeloglossum viride* var. *bracteatum* extract) in AlCl_3/D -galactose induced cognitive impairment mouse models, PD or genetic 5xFAD models with good neuroprotective effects (Li et al., 2021; Wu et al., 2021; Yu et al., 2019; Zhong et al., 2019). CE restores the levels of BDNF, FGF2 and their related signaling axes (including TrkB, p-Akt and Bcl-2) to alleviate neuronal death (Zhong et al., 2019). Moreover, we confirmed the detoxifying activity of Edaravone, a clinically used free radical scavenger in cerebral infarction, in a mouse model of Cd toxicity, eliminating oxidative stress, inflammation and alleviating inflammatory activation of microglia and astrocytes (Fan et al., 2021). Thus, the active chemicals may have potential therapeutic effect on AD.

Paeoniflorin (PF), a compound first isolated from *Paeonia lactiflora* Pall. in 1963 (Jiang et al., 2020), contains a plenty of pharmacological effects, including anti-myocardial ischemia, spasmolysis, neuroprotection, free radical scavenging, and immunomodulation (Tu et al., 2019), and no side-effects have been observed. In this study, we established a mouse model of Cd toxicity that, as previously, showed cognitive deficits mimicking an AD-like phenotype accompanied by multiple organic impairments (Fan et al., 2021). We then explored the protective effects of PF in Cd-intoxicated mice, by ameliorating their behavioral disorders and pathological changes, as well as the underlying molecular mechanisms. The activity of glutamate receptors, status of microglia and astrocytes, and neuronal synaptic markers PSD95 and synaptophysin in response to Cd or PF treatment were examined.

2. Materials and method

2.1. Animal

ICR mice (8 weeks, male, 40 in total) were provided by Beijing Vital River Laboratory Animal Technology Co., Ltd., under a license No. SYXK-2017-0005. Mice were randomly divided into 4 groups ($n = 10$), control, CdCl_2 (5 mg/kg), CdCl_2 (5 mg/kg) + PF (50 mg/kg), PF (50 mg/kg). The CdCl_2 was injected intraperitoneally every other day for 28 days. PF was administered by gavage once a day for 28 days, while saline was used in the control group. Animal experiments were carried out in accordance with the National Institutes of Health Laboratory Animal Care and Use Guidelines (NIH Publication No. 80-23) and approved by Animal Care and Use Committee of Minzu University of China.

2.2. Behavioral analysis

The Morris water maze (MWM) test was performed to determine the cognitive ability of mice and consisted of two phases of continuous experiments lasting 7 days (Zhong et al., 2019, Li et al., 2022). (1) Acquired training (first 6 days), to assess the learning ability of mice. (2) Probe trial (day 7 of the test) that used to assess the spatial memory ability of mice. In brief, animals were placed in a circular pool (110 cm in diameter and 50 cm in height) divided into four quadrants, with one quadrant placed with a platform (10 cm in diameter) submerged 1 cm of the water surface. A video-image system was placed above the center of the pool, which recorded the swimming path of the animals, which was then analyzed by software (Taimeng WMT-100). In acquired training (behavioral days 1–6), mice were allowed to find the platform freely within 1 min and the latency time was recorded. In probe trial (behavioral day 7), the platform was move away. The moved distance, residence time, and the crossing times of the animals in the target quadrant in the area where the original platform was placed, was recorded within 1 min.

The Y-maze spontaneous alternate experiment was used to test the animals' willingness to explore the new environments (Ren et al., 2021). The maze consisted of three equal length Y-shaped arms (30 cm long, 6 cm wide and 15 cm high) with an angle of 120° between them. Animals were allowed to explore freely from the top of one arm of the maze. Entry was considered when all four limbs of the animal were inside the arms. Correct spontaneous alternation occurred when the entering arm was different from the first two. The order in which the animal entered each arm over a 10-min period was recorded. Finally, the total alternation time and the number of spontaneous alternations were calculated.

A forced swimming test (FST) was performed to assess the depression-like phenotype of the animals (Yan et al., 2010). The experiment was performed in a transparent plastic cylindrical water tank (diameter 10 cm, height 38 cm). Water at $25 \pm 1^\circ\text{C}$ was poured into the tank (height 25 cm), the mice were gently placed above the water surface and then released for swimming for a 6-min swim. The first minute was set as an adaption and was not recorded. The next 5 min were recorded by software Taimeng FST-100. The immobility time of mice within these 5 min was calculated.

2.3. H&E staining and immunohistochemistry (IHC)

Mice were anesthetized with isoflurane, dissected, thorax opened, and the left ventricle was perfused with saline until the liver tissue turned white and the heart stopped beating. Hematoxylin-eosin (H&E) staining was performed for histological observation. In brief, sections were dewaxed with xylene and ethanol, stained with H&E staining solution (#G1003, Servicebio) and observed under a microscope (NIKON DS-U3). Prefrontal cortex, hippocampus and other brain tissues were embedded in paraffin, sectioned, antigen repaired, and then IHC stained. Astrocytes and microglia were detected by GFAP (1:100, # 168251-AP) and IBA1 (1:100, #10904-1-AP) specific antibodies purchased from Proteintech Group or Bioss. DAB (antigen positive expression) and hematoxylin (nuclear staining) signals were collected under a micro-

scope (NIKON DS-U3) and processed with Image Pro Plus 6.0 software (Media Cybernetics, Inc.).

2.4. Immunofluorescence

Brain sections were fixed in 4 % paraformaldehyde and dehydrated in 20 % and 30 % sucrose solutions. The sections were then washed 3 times with 1xPBS and sealed with 0.4 % Triton X-100 and 5 % goat serum (#SL038, Solarbio) for 2 h. After sealing and rinsed in 1xPBS for 3 times, sections were incubated with the primary antibody was incubated at 4°C overnight. The primary antibody is shown in Supplementary Table S1. After washed away the free primary antibody in 1xPBS for 3 times, the secondary antibody was incubated. The nuclei were stained with Hoechst33342. Images were taken with a TCS SP8 confocal microscope (Leica Microsystems, Germany).

2.5. Western blotting

The hippocampus and prefrontal cortex were dissected and proteins were extracted. Equal amount of proteins were loaded and separated by 10 % SDS-PAGE and then transferred to nitrocellulose membrane, sealed with 5 % skim milk for 1 h, washed 3 times with TBST, followed by incubation with primary antibody at 4 °C overnight. The antibodies used are shown in Supplementary Table S1. After incubation with the secondary antibody, images were developed by the Odyssey CLX infrared fluorescence scanning imaging system. The relative protein levels were normalized to β -actin based on the optical density of the blotted bands and quantified by Image J software.

2.6. RT-PCR

Total RNA was purified from brain tissue using TRIzol reagent (#15596018, Ambion) as previously described. First strand cDNA was reverse transcribed from 2.0 μ g RNA using EasyQuick RT MasterMix Kit (#CW 2019 M, Cowin Bio.) and then diluted in DEPC water at 1:10. Quantitative PCR were performed in a 10 μ L reaction on a Light Cycler 96 Real-Time PCR System (Roche) using 2x RealStar Green Fast Mixture (#A301-05, GenStar) containing primers (Supplementary Table S2) for IL-1 β , IL-6, TNF- α , IFN- γ , and IL-10, respectively. Three replicates for each template were performed and five samples were examined.

2.7. Statistical analysis

All data were expressed as mean \pm s.e.m. One-way or two-way Analyses of Variance (ANOVA) were performed to examine the significance of differences between groups and are indicated separately in each figure. Otherwise, Mann Whitney *U* test was performed for nonparametric analysis. $p < 0.05$ was considered significant.

3. Results

3.1. PF attenuates Cd-induced systemic toxicity in ICR mice

To determine the effectiveness of PF (Fig. 1A) in reducing the toxicity of Cd, ICR mice were exposed to intraperitoneally

administered Cd for 28 days (Fig. 1B) or while being given PF treatment. During the experiment, mice were weighted on days 1, 14 and 28. As shown in Fig. 1C, mice in the control or PF group gained normal body weight over the same period, indicating that PF was not toxic to mice (Fig. 1C, PF group). However, mice treated with Cd lost significantly more weight compared to the control group, especially on day 28 ($p < 0.01$), while mice treated with Cd + PF loss less weight ($p < 0.05$). In addition, increased proteins were detected in the urine collected on day 28. The results showed that Cd significantly increased urinary protein in mice, indicating that Cd toxicity disrupts the integrity of the kidney (Fig. 1D). Consistently, kidney atrophy was observed at the end of the experiment after dissection of the organs, as the kidney index (organ weight/body mass) decreased (Fig. 1E, kidney, $p < 0.001$). In addition, hepatomegaly and encephalomegaly was found as the liver and brain indices increased (Fig. 1E, liver and brain, $p < 0.001$). Again, PF treatment protected organs from Cd-induced toxicity and recovered them to normal. Furthermore, we performed H&E staining on sections of liver, kidney, small intestine and testis and found that the toxicity of Cd induced severe damage but was alleviated by PF treatment (Fig. 1F). Normally, hepatocytes were arranged radially around the central vein without dilatation and congestion, inflammatory cell infiltration and other pathological changes. However, in Cd-intoxicated mice, the hepatocytes were irregularly arranged with blurred hepatic cord boundaries and inflammatory cell infiltration around the central vein (Fig. 1F, liver in Cd group). In contrast, in Cd + PF treated mice, hepatocytes were neatly aligned and inflammation was alleviated, indicating PF-mediated protection of the liver from Cd-induced toxicity. Similarly, renal cells were tightly arranged with well-defined tubular lumen and glomerular structure. After Cd toxicity, renal cells were loosely arranged with marked swelling, narrowed tubular lumen and irregular glomeruli (Fig. 1F, kidney with Cd). Again, the above abnormalities were ameliorated by PF. In addition, Cd-induced toxicity to the small intestine and testes was attenuated by PF treatment. Notably, Cd toxicity was clearly observed as manifested by atrophy of spermatogonial epithelial cells and a dramatic reduction in spermatocyte numbers (Fig. 1F, testis with Cd). In other words, Cd was able to effectively penetrate the testicular barrier in the blood and induce toxicity. Fortunately, PF is also effective in mitigating the toxicity of Cd in the testis (Cd + PF). Thus, PF is a potential natural product to attenuate the toxicity of Cd in ICR mice.

3.2. PF alleviates the AD-like and depression-like phenotypes induced by Cd toxicity in ICR mice

Behavioral tests were performed on ICR mice after modeling and drug treatment. A Y-maze test was performed to determine the willingness of mice to explore new environments. We found that Cd-intoxication reduced the willingness of mice to explore new environments, but could be restored by PF treatment (Fig. 2A). In addition, Cd-intoxication induced a depression-like phenotype in mice, as determined by the forced swimming test (FST) (Fig. 2B). In the test, Cd-induced immobility was significantly prolonged in the FST, while PF treatment reduced the duration of immobility, indicating an improvement in Cd toxicity ($p < 0.001$).

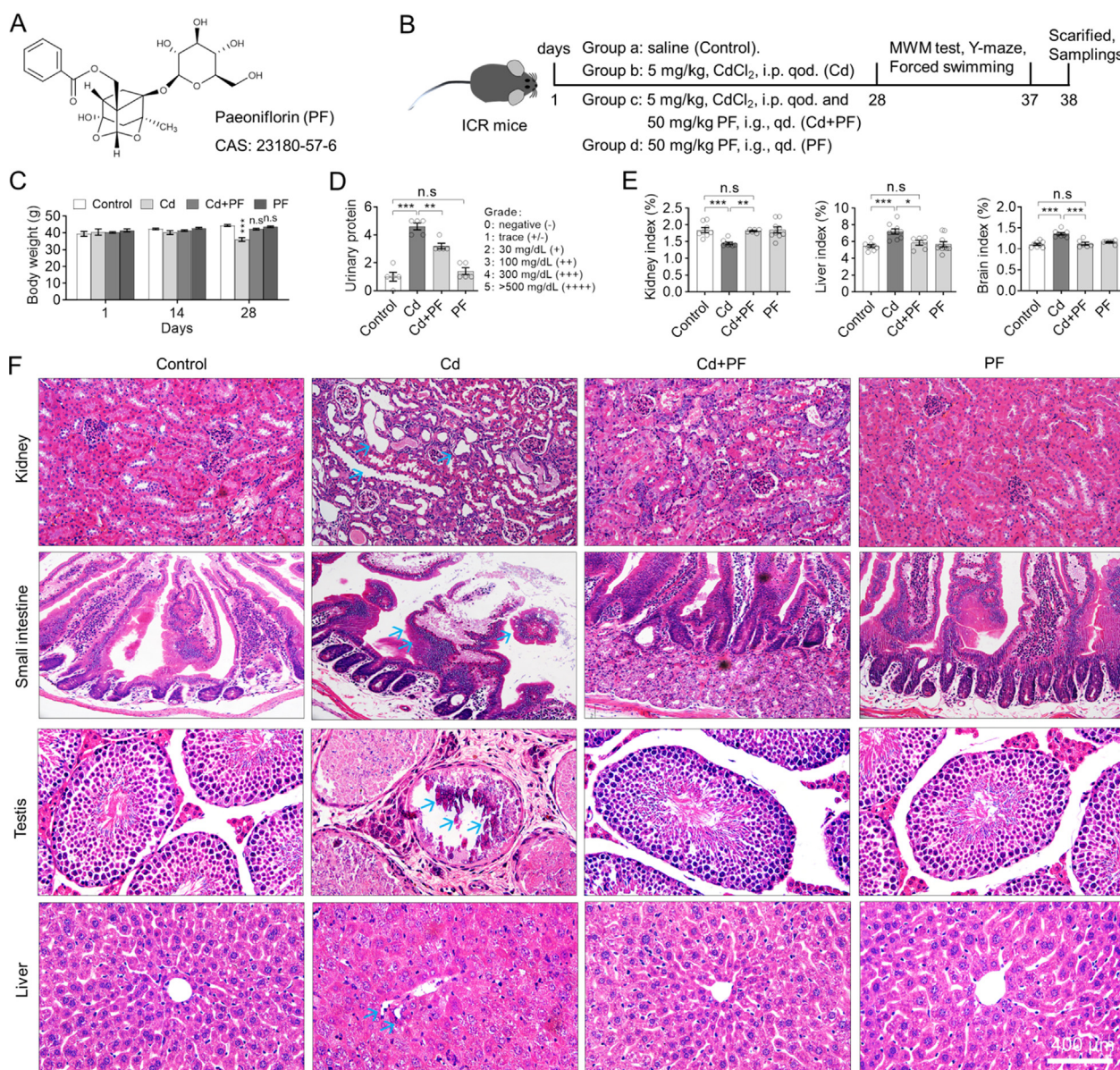


Fig. 1 Cd induced systemic injury in ICR mice but can be attenuated by PF treatment. (A) Chemical structure of Paeoniflorin (PF). (B) Timing of animal experiments. i.p. qod., intraperitoneally injection, every other day. i.g. qd., injection by gavage, once daily. (C) Body weight of mice. PF prevented the weight loss of Cd-treated mice. (D) PF reduced the abnormal increase in urinary protein caused by Cd toxicity. (E) Organ indices of liver, kidney and brain. Cd-induced toxicity caused hepatic edema, cerebral edema, and renal atrophy according to organ/body mass index. (F) H & E staining was used to observe the toxicity of Cd in different organs and the protection PF against Cd-induced toxicity. Arrows indicate morphological changes in Cd-treated tissues. In this figure, C, two-way ANOVA, post hoc Tukey's test was performed. In D, a nonparametric analysis was performed by the Mann-Whitney *U* test. In E, a one-way ANOVA, post hoc Dunnett's test was performed. n.s, not significant; *, $p < 0.05$; **, $p < 0.01$; ***, $p < 0.001$.

In MWM experiments, we carried out acquired training (last 6 days) and probe trail successively. During acquired training, mice were allowed to find the platform submerged in water. During training, the mice acquired a memory for the platform position, so the time to find the platform (escape latency) gradually decreased with training (Fig. 2C, control). However, Cd-intoxication impaired the mice's memory, so it took longer to find the platform compared to the control (Fig. 2C, Cd). In contrast, PF treatment maintained the learning and memory abilities of the mice, similar to the controls,

indicating the attenuation of Cd-toxicity (Fig. 2C, Cd + PF). Recording of swimming occupancy plot also showed that the route to find the platform was much more complicated in Cd-intoxicated mice compared to the other groups (Fig. 2D). Moreover, mice did not differ significantly in the MWM test, indicating that Cd or PF did not affect the physiological movements of mice (Fig. 2C, right column). Consistently, after completion of acquired training, probe trail was performed in which the platform was removed and mice were allowed to swim in the maze for 1 min and the swimming

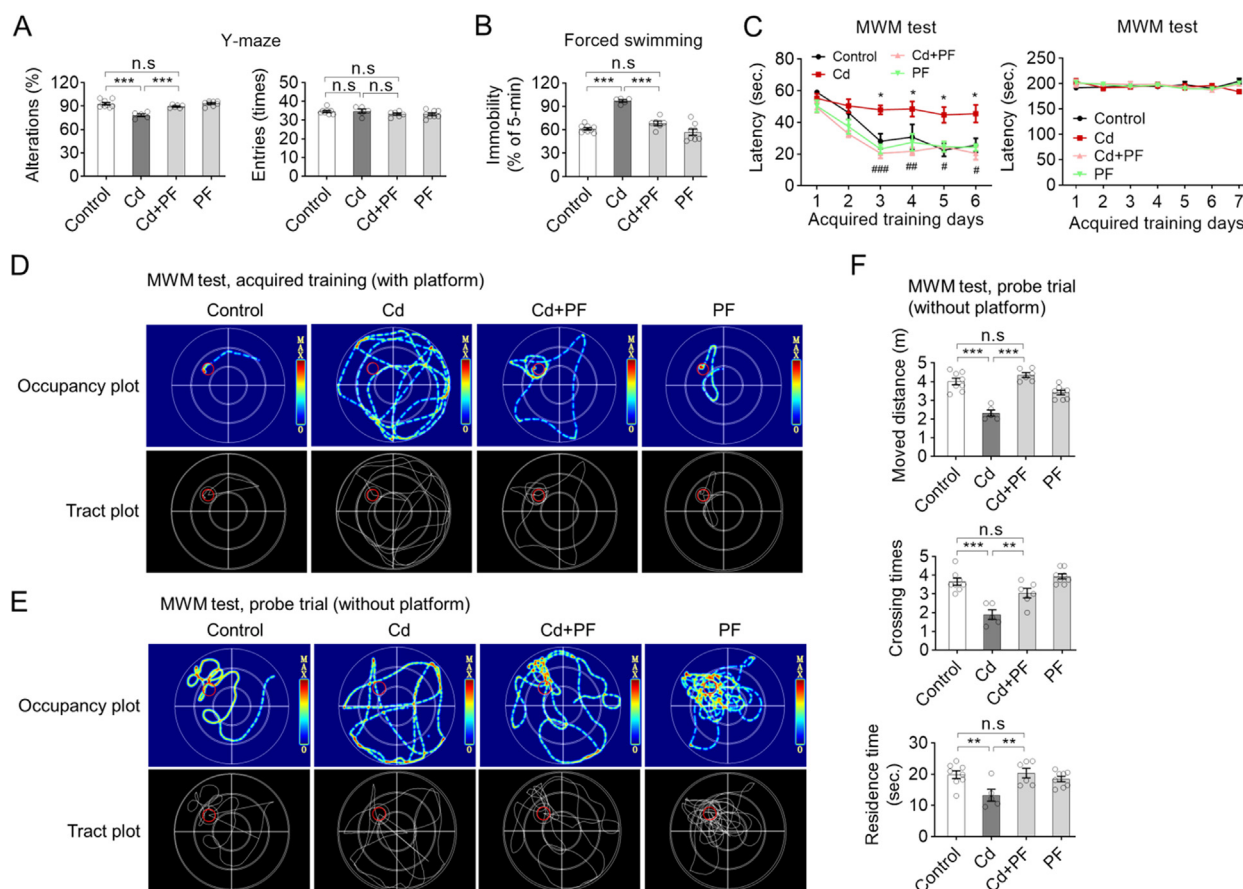


Fig. 2 Cd-intoxication induced AD-like and depressive-like behaviors in ICR mice, but can be restored by PF treatment. (A) Spontaneous alterations and number of entries in the Y-maze test in mice. (B) Mice in the Cd group exhibited longer immobility time in the FS test, indicating a depressive-like phenotype; which was ameliorated by PF treatment. (C) Escape latency (with platform) in ICR mice in the acquired training test. (D-E) Representative swim paths and thermal-infrared trajectories for MWM tests obtained on behavioral days 6 and day 7, respectively. The location of the underwater platform is marked with a red circle to represent the target area. (F) Probe trail of MWM tests (day 7) showing distance traveled, residence time and number of crossings in the target quadrant where the platform was originally placed. In this figure, in A-B and F, a one-way ANOVA, post hoc Dunnett's test was performed. In C left panel, two-way RM ANOVA, post hoc Tukey's test was performed. n.s., not significant; *, $p < 0.05$; **, $p < 0.01$; ***, $p < 0.001$ (Cd vs Control); ##, $p < 0.01$, ###, $p < 0.001$ (Cd + PF vs Cd).

path was recorded (Fig. 2E). We found that in the control, PF and Cd + PF groups, mice spent most of their time in the quadrant where the platform was initially placed, with the exception of the Cd-treated group. Statistical analysis of swimming paths also confirmed that Cd-treated mice spent less time in the target quadrant area, traversed it less frequently and moved a greater distance than the control and even the Cd + PF group (Fig. 2F). In conclusion, Cd intoxication caused cognitive dysfunction in mice, which could be restored by PF treatment (Fig. 2).

3.3. PF reduces Cd toxicity in mice by recovering the activity of glutamate receptors

The glutamate ionotropic receptor NMDA regulates learning and long term potentiation in the brain. To study whether Cd toxicity affects NMDA receptor activity and to examine the protective role of PF, the activity of NMDA receptor 2A and 2B was detected by immunofluorescence and Western blotting using antibodies specific for their phosphorylation

(Fig. 3, Fig. S1). As shown in Fig. 3A, p-NMDA receptors (2B) were clearly expressed on the surface of cell membrane and in the cytoplasm of hippocampal and prefrontal cortex neurons. However, p-NMDAR2B was reduced after Cd treatment compared with controls (Fig. 3A, p-NMDAR). After PF treatment, the levels of p-NMDAR2B were recovered in the Cd + PF group. Western blotting also confirmed the restoration of protein levels of these receptors (Fig. 3B and C).

Other important types of GluRs are AMPA receptors, of which GluR1 and GluR2 are the two main subtypes, both of which are regulated by protein phosphorylation (Steinberg et al., 2006, Lee et al., 2010). In the experiment, phospho-GluR2 (p-GluR2) decreased after Cd treatment compared to the control (Fig. 3A, p-GluR2), and also confirmed by Western blotting in the Cd-treated samples (Fig. 3B and C). In contrast, p-GluR1 was up-regulated after Cd treatment. These results imply that Cd-intoxication induced the destruction of GluRs in the CNS. However, PF treatment restored the Cd-induced changes in GluR1 and GluR2, attenuating Cd toxicity (Fig. 3, Cd + PF).

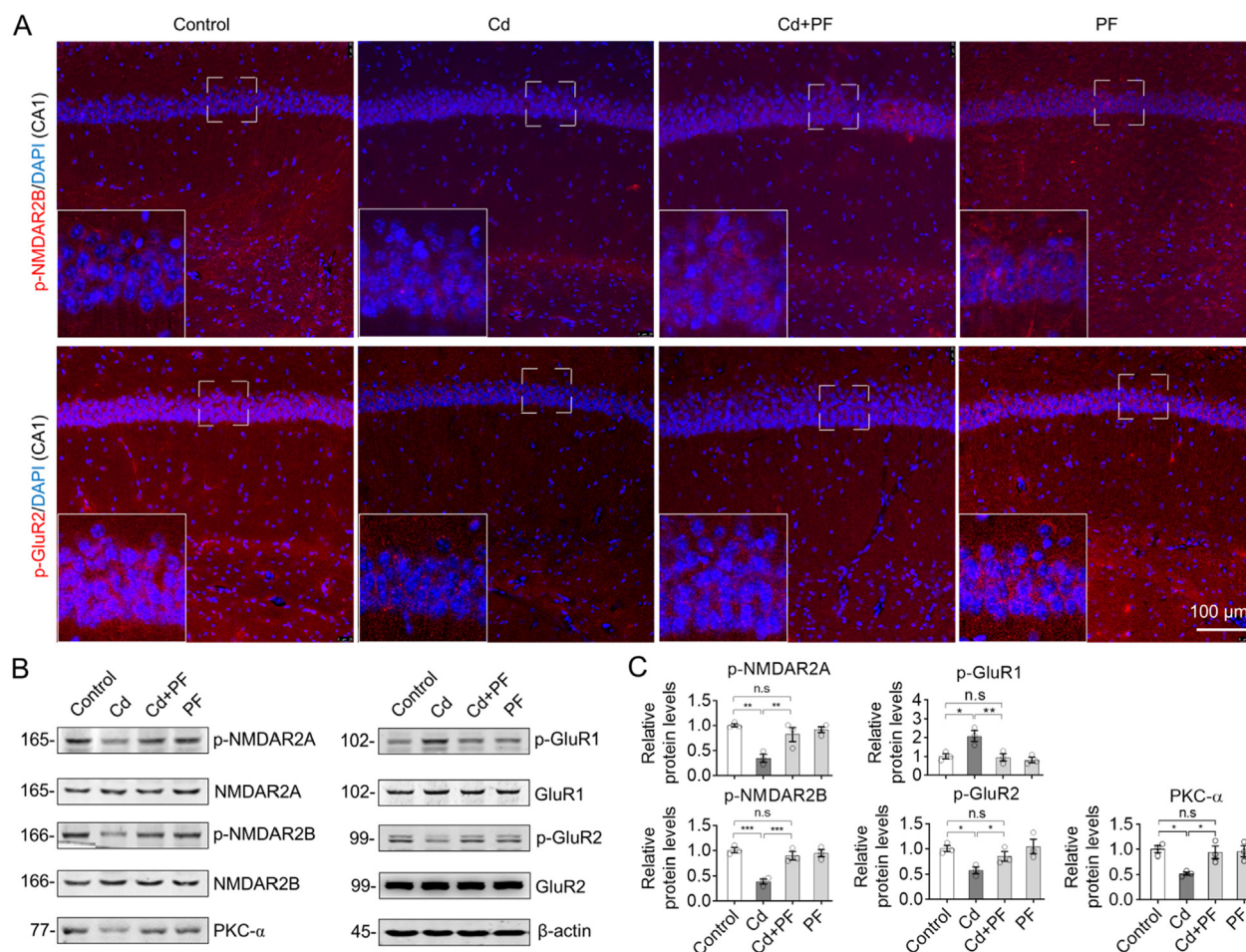


Fig. 3 PF recovered the activity of glutamate receptors in response to Cd-induced toxicity. (A) Representative immunofluorescence images of phospho-NMDAR2B and phospho-GluR2 in brain sections of ICR mouse. Images of hippocampal area DG and prefrontal cortex (PFC) are shown in Supplementary Materials Fig. S1. (B) Protein levels in the hippocampus were detected by Western blot analysis. (C) Quantification of relative protein levels as indicated by blot intensity in (B) by Image J software. One-way ANOVA, post hoc Tukey's test was carried out. n.s., not significant; *, $p < 0.05$; **, $p < 0.01$; ***, $p < 0.001$.

3.4. PF attenuates Cd-induced gliosis in ICR mice

The status of microglia and astrocytes was detected, as they are the major regulators of neuroinflammation in the CNS. Immunofluorescence (IF) staining of brain slices from the hippocampus and prefrontal cortex were performed using antibodies specific to GFAP and IBA1 (Fig. 4). The signal and number of microglia (IBA1) and astrocytes (GFAP) in hippocampal DG, CA1 and cortex (PFC) were significantly increased after Cd treatment (Fig. 4A and B, Fig. S2). Under Cd-induced toxicity, gliosis was activated, as evidenced by the enlargement of cell bodies and lengthening of protrusions. In contrast, the number of microglia and astrocytes decreased with PF treatment. Consistently, protein levels examined by Western blotting confirmed opposite changes of GFAP and IBA1 in response to Cd and PF as revealed by IF (Fig. 4C). Furthermore, we performed IHC staining of brain slices. We found that Cd induced toxicity increased the number of GFAP and IBA1-positive cells in the DG, CA1 and CA3 regions of the hippocampus and in the prefrontal cortex, whereas PF effectively reduced the increase in these cells (Fig. 5, Fig. S3).

Consistently, the results of RT-PCR to determine the expression of inflammatory factors such as IL-1 β , IL-6, TNF- α , as well as IFN- γ and anti-inflammatory factor IL-10 also confirmed the anti-inflammation effect of PF (Fig. 5D). Thus, PF effectively alleviated Cd-induced gliosis.

3.5. PF alleviates Cd-induced gliosis by reducing HIF-1 α levels and protecting neurons

HIF-1 α is involved in cellular adaptation to oxidative stress and regulates inflammation (Ashok et al., 2017). Therefore, we performed co-immunostaining of HIF-1 α with GFAP, as shown in Fig. 6. HIF-1 α was mainly expressed in the cytoplasm. After Cd intoxication, the level of HIF-1 α was significantly increased, along with a plenty of activated astrocytes, as shown by GFAP-labeling (Fig. 6A, Fig. S4). Compared to controls, astrocytes were activated and their number increased after Cd-treatment, whereas PF attenuated the toxicity of Cd and reduced the increment of HIF-1 α and the activation of astrocytes. We also confirmed that neuronal responses to Cd and PF treatment were opposite to the changes in astrocytes

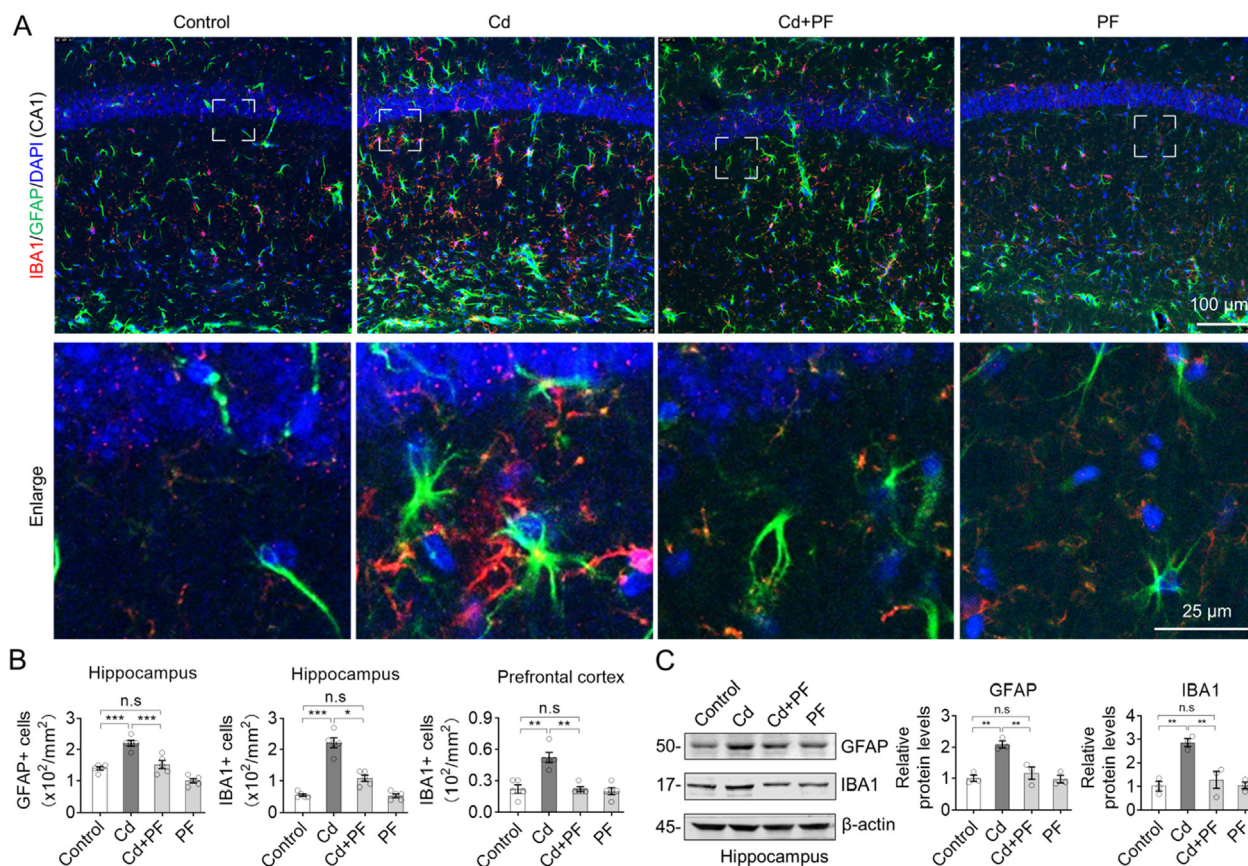


Fig. 4 Representative immunofluorescence images and blots of GFAP and IBA1. (A) Cd-induced toxicity in the brain was manifested by an increase in GFAP- and IBA1-positive cells, indicating activation of microglia and astrocytes. However, PF treatment attenuated the Cd-induced neurotoxicity and restored cellular homeostasis. Regional images of hippocampal DG and prefrontal cortex (PFC) are shown in Supplementary Material Fig. S2. (B) Cell counts were calculated from the images. (C) Western blots analysis of GFAP and IBA1 protein levels. In B-C, one-way ANOVA, post hoc Dunnett's test were performed. n.s, not significant; *, $p < 0.05$; **, $p < 0.01$; ***, $p < 0.001$.

(Fig. 6B, Fig. S4). In detail, Cd toxicity disrupted the activity of neurons and even caused substantial loss of neurons, especially in hippocampus (Fig. 6B, Fig. S4), by staining neurons with specific antibodies to the protein marker MAP2, an important cytoskeletal protein that is closely related to neuroplasticity and plays an important role in dendritic and branchial extension (Lingwood et al., 2008). However, PF treatment prevented Cd-induced loss of neurons and maintained CNS homeostasis. Western blotting of protein levels of HIF-1 α and MAP2 also showed results consistent with immunofluorescence staining (Fig. 6C).

In addition, the reduction of postsynaptic densifying membrane 95 (PSD95) and synaptic vesicle protein (synaptophysin) in brain tissues of AD patients is closely correlated with the degree of cognitive decline (Qin et al., 2004, Tajiri et al., 2013). We found that PSD95 and synaptophysin were significantly reduced following Cd treatment (Fig. 6C), implying impairment of neuronal synaptophysin by Cd toxicity. However, consistent with the maintenance of neurons by PF treatment, protein levels of PSD95 and synaptophysin were restored. In other words, PF attenuated Cd-induced neuronal damage and protected neurons, especially by restoring synaptic plasticity.

At the mechanistic level, we also explored molecular changes within microglia. CD68 (also named macrogladin in

mice) is a lysosomal membrane protein that is highly expressed by macrophages and activated microglia, but less so by resting microglia, as it is essential for lysosomal activity of microglia to clear damaged cellular components or molecules. It is therefore positively correlated with pathological and cognitive function in AD (Minett et al., 2016). Using immunofluorescence, we found co-localization of microglia (stained by IBA1) with CD68 (Fig. 7), especially in Cd-intoxicated brain samples, indicating microglia activation and upregulation of CD68. It can be seen that this is a stress response of the mouse brain to Cd toxicity, and is very similar to the pathological features of AD. This result is also consistent with the behavioral manifestations of the mice described previously. That is, the cognitive impairment induced by Cd toxicity corresponds to a series of changes in glial cells and neurons. However, PF treatment again effectively attenuated the toxicity of Cd and alleviated the increase in CD68, indicating a reduction in lysosomal activity in microglia. In other words, PF protected neurons from Cd-induced toxicity and maintained CNS homeostasis (Fig. 8).

4. Discussion

It is hypothesized that the transitory deposition of amyloid- β protein (A β) arises from the metabolic imbalance of A β pro-

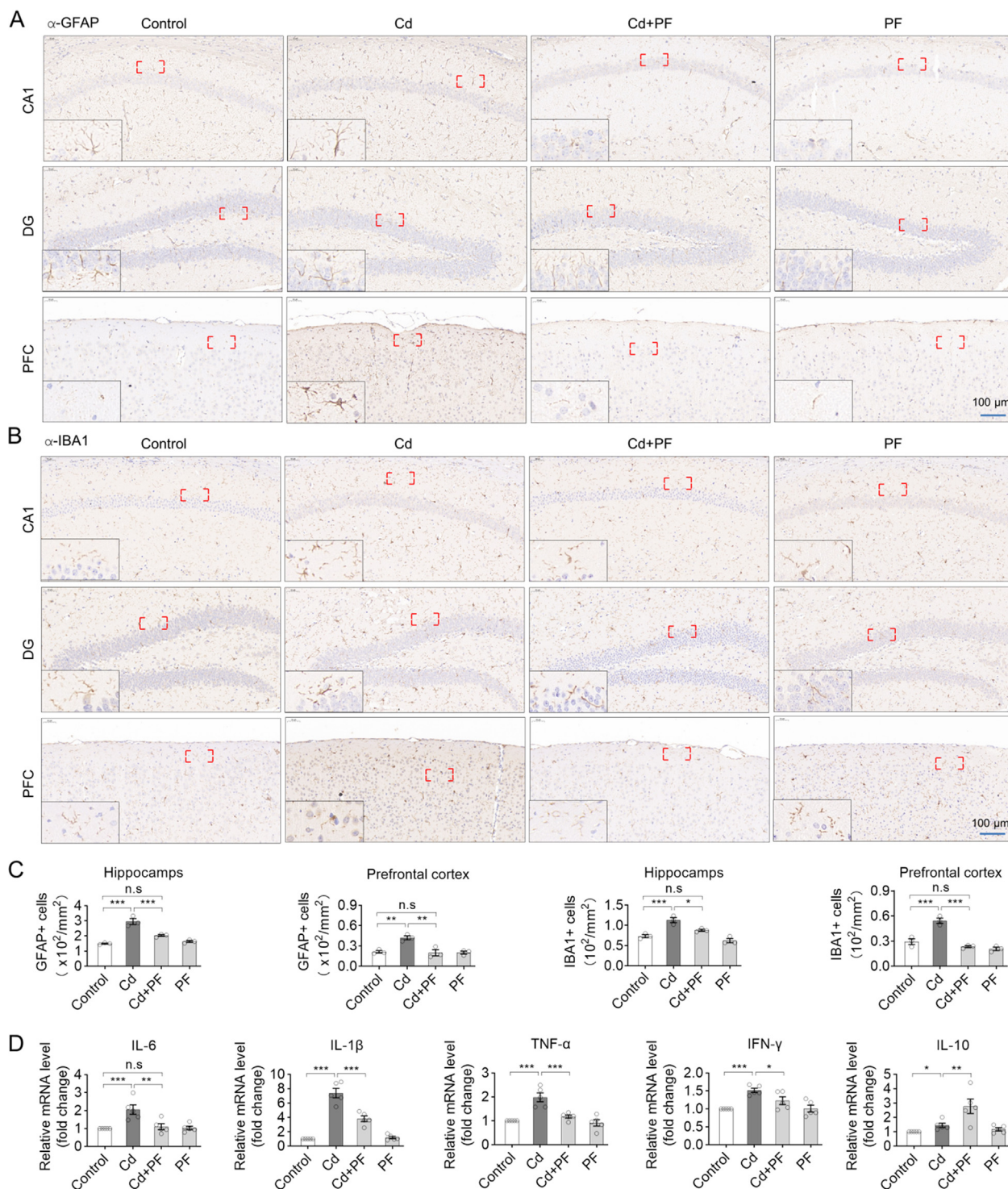


Fig. 5 Immunohistochemical staining of GFAP and IBA1 in the prefrontal cortex (PFC) and hippocampus. (A-B) Representative IHC images show that Cd-induced toxicity activated the inflammatory response in astrocytes and microglia, as indicated by the increased levels of GFAP and IBA1. However, PF restored Cd-induced inflammation. Images of GFAP and IBA1 in hippocampal CA1 are showed in Supplementary Materials Fig. S3. (C) Statistical analysis of the number of GFAP- and IBA1-positive cells in the hippocampus and prefrontal cortex was performed. (D) The mRNA expression levels of inflammatory factors in brain tissue were determined by RT-PCR. In C and D, a one-way ANOVA, post hoc Dunnett's test was performed. n.s., not significant; *, $p < 0.05$; **, $p < 0.01$; ***, $p < 0.001$.

tein and the formation of senile plaques, which are the essential factors for development of AD (Das et al., 2003, Jonsson et al., 2013, Liang et al., 2020). Environmental toxic metal such as

Cd penetrates the BBB and eventually accumulates in the brain, causing neurotoxicity, mainly by inducing the activation of various signaling pathways involved in inflammation,

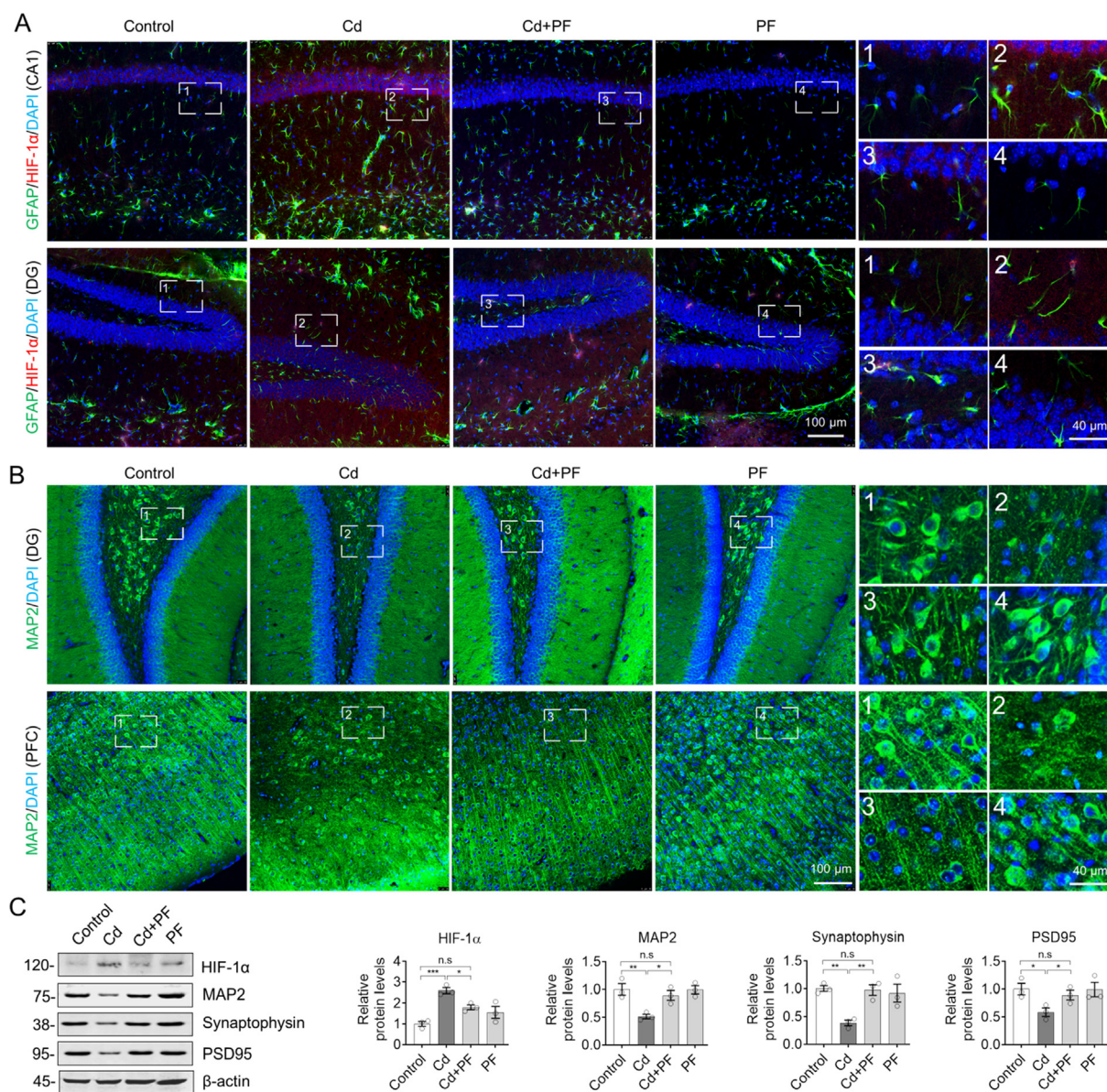


Fig. 6 PF inhibited Cd-induced inflammation and protected neurons by attenuating the increase of HIF-1 α . (A) Immunofluorescence staining of GFAP and HIF-1 α in the hippocampus. Cd induced an increase in HIF-1 α levels and the number of GFAP-labeled astrocytes. PF mitigated the increase in HIF-1 α expression and astrocyte activation, thereby reducing inflammation. (B) Immunofluorescence staining for MAP2 in PFC and hippocampus. Images of hippocampal CA4 (A) and CA1 (B) are shown in Supplementary Materials Fig. S4. (C) Western blotting for protein levels of GFAP and HIF-1 α as well as the neuronal synaptic proteins synaptophysin and PSD95 in the hippocampus. The intensity of the blotted bands was quantified using Image J software. One-way ANOVA, post hoc Dunnett's test was performed. n.s, not significant; *, $p < 0.05$; **, $p < 0.01$; ***, $p < 0.001$.

oxidative stress, and neuronal apoptosis (Yuan et al., 2013, Qadir et al., 2014, Peng et al., 2017, Wu et al., 2021). Abnormal deposits of toxic metals such as Cadmium and Al in the plaques formed by A β deposition, consistent with the increased number and size of A β plaques in AD transgenic APP/PS1 mice after Cd exposure in drinking water. Cd ions interact with A β to promote plaque formation and aggregation. In addition, blood Cd levels are significantly associated with AD-related mortality in the elderly (Li et al., 2012, Min and Min 2016, Huat et al., 2019). There is also evidence that Cd levels in the blood and hair of AD patients are significantly

higher than those of healthy controls (Li et al., 2012). The above results indicate that toxic metal contamination is closely related to the occurrence of AD.

Previously, we preliminarily investigated the relationship between toxic metals and AD in a mouse model poisoned with AlCl₃ combined with D-galactose (Gal), and confirmed that AlCl₃/Gal caused AD-like symptoms of learning and memory impairment (Zhong et al., 2019). Similarly, mice treated with Cd alone showed cognitive deficits and behavioral decline (Fan et al., 2021). Moreover, Cd- and Al-mediated neurotoxicity was associated with decreases in neurotrophic factors

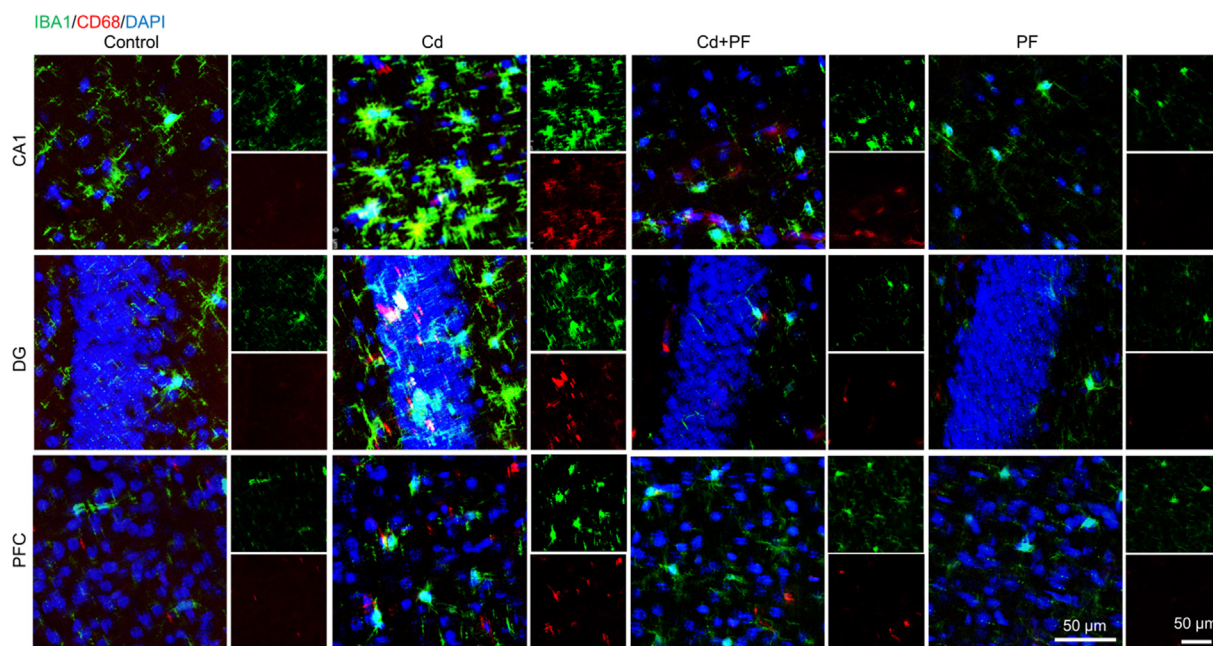


Fig. 7 Immunofluorescence staining of IBA1, CD68 in prefrontal cortex (PFC) and hippocampus. (A) Cd toxicity activated microglia, as indicated by increased levels of CD68 and number of IBA1-positive cell. PF attenuated Cd toxicity, microglia activation and the increase of CD68.

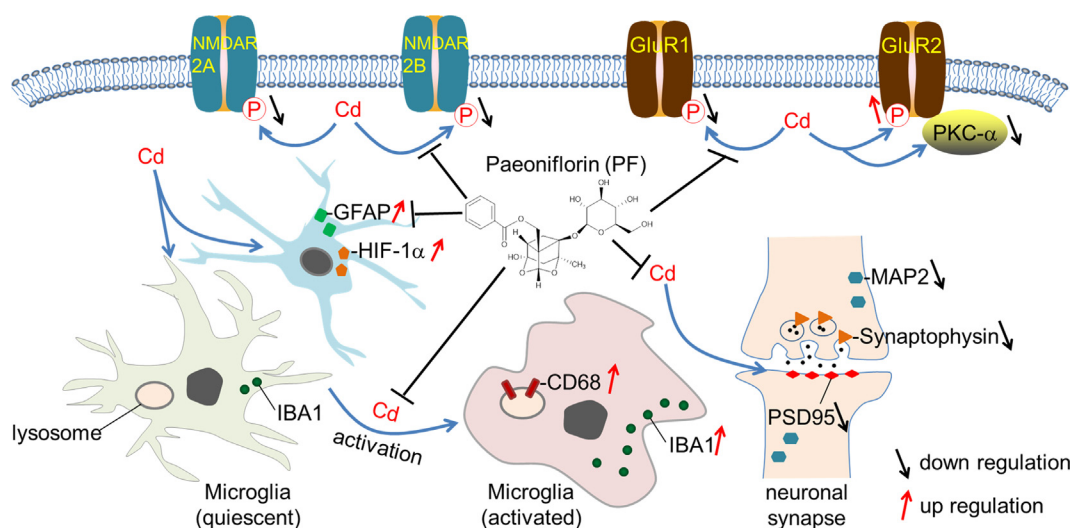


Fig. 8 Schematic graph showing PF-mediated attenuation of Cd toxicity and restoration of homeostasis in the brain.

such as BDNF and FGF2, and increased oxidative stress and inflammation, and even the DNA damage response (Zhang et al., 2019). These phenomena are very similar to the phenotypes of 5xFAD mouse. With these models, we determined the antioxidant and neuroprotective of natural chemicals such as THSG, CE (Zhong et al., 2019). CE was used to treat 5xFAD mice in the early stage and was found to be effective in improving cognitive dysfunction in AD model mice (Li et al., 2021), even in mouse directly intracerebral injected of A β . In this study, PF could significantly reduce AD-like behavior in Cd-intoxicated mice (Fig. 2).

Cd-intoxicated mice exhibited learning and memory disorders, which may be related to abnormal glutamate receptor

function. Our results showed that Cd down-regulated the activity of NMDA receptors (2A and 2B) and inhibitory glutamate receptor GluR2, and up-regulated the phosphorylation of excitatory glutamate receptor GluR1, while PF could restore the aforementioned protein changes (Fig. 3). It is possible that Cd-induced destruction and loss of synapses lead to a compensatory increase in GluR1 and its phosphorylation in the remaining synapses, with GluR1 being the most common subunit. These results indicate that Cd neurotoxicity induces dysfunction of glutamate receptors, but can be restored by PF via maintaining the homeostasis of glutamate receptors (Fig. 3). Glutamate is the most important excitatory neurotransmitter in the CNS, regulating neuronal growth and differ-

entiation, synaptic plasticity and transmission, and learning and memory. It acts broadly on two types of receptors: ionotropic and metabotropic. The former includes NMDA receptors (NMDAR), AMPA receptors (AMPA) and kainate receptors (KAR), and the latter are mGluRs. NMDAR is a postsynaptic receptor essential for glutamate-mediated synaptic transmission, which mediates Ca^{2+} influx and activates its downstream cascade reactions to mediate information processing and storing. NMDAR consists of two NR1 subunits and two NR2 subunits. In the hippocampus, the NR2 subunits are mainly expressed as NR2A and NR2B. The composition and location of the NMDAR subunits determine neuronal fate (Hettinger et al., 2018). The AMPAR mediates rapid excitatory synaptic transmission in the CNS, and its dynamic expression in the postsynaptic membrane is related to the induction and maintenance of long-term potentiation (LTP) and depression (LTD), and regulates learning and memory activity. Excessive endocytosis and cleavage of AMPAR under the action of A β leads to loss of postsynaptic membrane, thereby lead to synaptic damage and dysfunction, as well as subsequent cognitive impairment in the early stage of AD (Lee et al., 2010, Lüscher and Malenka 2012, Marcondes et al., 2020). Aberrant expression of NMDAR and AMPAR induced by excessive A β is associated with the occurrence of AD. Binding of A β oligomer to substrates of GluR2 has been reported to induce an acute increase in calcium-permeable AMPAR and inhibit LTP, resulting in a decline of synaptic plasticity (Abd-Elrahman et al., 2021). NMDAR activation bidirectional modulates A β levels: low concentrations of NMDA increase A β levels by increasing presynaptic endocytosis, while high concentrations of NMDA reduce A β production by dendritic calcium-dependent signaling and increase α -secretase activity (Hettinger et al., 2018). While A β protein is deposited, it affects proteins involved in the LTP effect in the hippocampus, and inhibiting its induction and reducing the patient's ability of learning and memory.

Microglia are the major immune cells in the CNS that recognize and remove damaged nerves, plaques and infectious substances, and maintain homeostasis (Reiner and Levitz 2018). However, prolonged activation of microglia releases excessive inflammatory factors and oxidative active substances, triggering inflammatory responses that lead to neuronal damage, and thus neurotoxicity. A plenty of activated microglia were found in the brains of APP transgenic mice and AD patients, and inflammatory factors such as IFN- γ , TNF- α , IL-1 β and IL-6 were significantly increased, indicating the presence of inflammation. Toxic A β and Tau proteins are thought to activate microglia in the brain via binding to receptors on the surface of the microglia and triggering their activation. Activated microglia release cytokine and chemokine, reactive oxygen species and other toxic substances, such as NO, tumor necrosis factor, superoxide, etc., evoke inflammation, consistent to the existence of inflammation in AD patients (Magee and Grienberger 2020). Triggering receptor expressed on myeloid cells 2 (TREM2), a receptor widely expressed on the surface of microglia, recognizes damage-associated molecular patterns (DAMPs), which activates microglia and trigger neuroinflammation (Jonsson et al., 2013). Damaged neurons release DAMPs, which bind to TREM2 and activate microglia, which secrete a flood of inflammatory cytokines and free radicals, further damaging neurons and accelerating the progression of AD (Wilkins

et al., 2015) Thus, the pathogenesis of AD is accompanied by a cycle of inflammation that, when it occurs, causes widespread neuronal cell dysfunction and abnormal death. Suppression of inflammation is important for the clinical management of AD (Steinberg et al., 2006, Qu et al., 2021). Consistently, we show that Cd toxicity induces microglia and astrocyte activation, which can be attenuated by PF treatment, possibly by attenuating the upregulation of HIF-1 α and CD68 as they are associated with microglia phagocytosis. HIF-1 α is a major transcriptional regulator of the adaptive response to hypoxia, by binding to the core DNA sequence 5'-TACGTG-3' within the promoter of the target genes (Wang et al., 2021). HIF-1 α is upregulated in activated microglia, which may contribute to the subsequent pro-inflammatory state. Furthermore, activation of HIF-1 α signaling in microglia correlates with disease severity, with particularly high HIF-1 α levels in plaque-associated microglia. However, inhibition of HIF-1 α can alter the phenotype of microglia, leading to an increase in the number of microglia surrounding amyloid- β plaques, thereby protecting neurons (Wendeln et al., 2018).

Synaptic plasticity is essential for central nerve regeneration and plays an irreplaceable role in cognitive regulation (Citri and Malenka 2008). The massive loss of neurons and synapses in the hippocampus observed in AD patients is due to the accumulation of NFT and Tau proteins and the presence of senile plaques caused by the accumulation of A β . Thus, with the development of AD, the accumulation of A β oligomers produces changes in the expression of proteins that regulate synaptic function (Skaper et al., 2017, Cuestas Torres and Cardenas 2020). MAP2 was originally found to bind and stabilize microtubules. Synaptic loss in the hippocampus and cortex is an early event in cognitive dysfunction. A series of structural changes in the hippocampus underlie AD and cognitive deterioration, particularly a reduction in synaptic density. MAP2 is involved in maintaining the structural integrity of the neuronal cytoskeleton and synaptic plasticity (Citri and Malenka 2008, Lingwood et al., 2008, Bodakuntla et al., 2019). In addition, PSD95 interacts with, stabilizes, and is transported to the postsynaptic membrane via NMDAR and AMPAR and is a major regulator of synaptic maturation. PSD95 abnormality is associated with cognitive and learning disabilities (Coley and Gao 2018). Also, the loss of synaptophysin in the brain is closely related to the degree of cognitive decline in AD patients (Sweatt 2001, Qin et al., 2004). Therefore, by detecting synaptic associated proteins (MAP2, PSD95 and synaptophysin), we found that Cd toxicity not only reduces the number of neurons, but also destroy their structure, especially in the CA1 region, and down-regulated the expression of MAP2, PSD95 and synaptophysin. In summary, the toxicity of Cd impairs glutamate receptors, synaptic proteins and cause inflammatory response in the nervous system, while PF can maintain the function of glutamate receptor, repairs the synaptic plasticity, inhibits activation of glial cells, nerve inflammation, and thereby exerts its neuroprotective effect.

Declaration of Competing Interest

The authors declare that they have no known competing financial interests or personal relationships that could have appeared to influence the work reported in this paper.

Acknowledgments

Thanks to the National Natural Science Foundation of China (81873088), the MUC 111 project (URTP2017110030) and SZU Top-Ranking project (860000210) for financial support.

Appendix A. Supplementary material

Supplementary data to this article can be found online at <https://doi.org/10.1016/j.arabjc.2022.104406>.

References

- Abd-Elrahman, K.S., Sarasija, S., Ferguson, S.S.G., 2021. The role of neuroglial metabotropic glutamate receptors in Alzheimer's disease. *Curr. Neuropharmacol.* <https://doi.org/10.2174/1570159X19666210916102638>.
- Ashok, B.S., Ajith, T.A., Sivanesan, S., 2017. Hypoxia-inducible factors as neuroprotective agent in Alzheimer's disease. *Clin. Exp. Pharmacol. Physiol.* 44, 327–334. <https://doi.org/10.1111/1440-1681.12717>.
- Bodakuntla, S., Jijumon, A.S., Villablanca, C., et al, 2019. Microtubule-associated proteins: structuring the cytoskeleton. *Trends Cell Biol.* 29, 804–819. <https://doi.org/10.1016/j.tcb.2019.07.004>.
- Chin-Chan, M., Navarro-Yepes, J., Quintanilla-Vega, B., 2015. Environmental pollutants as risk factors for neurodegenerative disorders: Alzheimer and Parkinson diseases. *Front. Cell Neurosci.* 9, 124. <https://doi.org/10.3389/fncel.2015.00124>.
- Citri, A., Malenka, R.C., 2008. Synaptic plasticity: multiple forms, functions, and mechanisms. *Neuropsychopharmacology* 33, 18–41. <https://doi.org/10.1038/sj.npp.1301559>.
- Coley, A.A., Gao, W.J., 2018. PSD95: a synaptic protein implicated in schizophrenia or autism? *Prog. Neuropsychopharmacol. Biol. Psychiatry.* 82, 187–194.
- Cuestas Torres, D.M., Cardenas, F.P., 2020. Synaptic plasticity in Alzheimer's disease and healthy aging. *Rev. Neurosci.* 31, 245–268. <https://doi.org/10.1515/revneuro-2019-0058>.
- Das, P., Howard, V., Loosbrock, N., et al, 2003. Amyloid-beta immunization effectively reduces amyloid deposition in FcRgamma-/- knock-out mice. *J. Neurosci.* 23, 8532–8538.
- Fan, S.R., Ren, T.T., Yun, M.Y., et al, 2021. Edaravone attenuates cadmium-induced toxicity by inhibiting oxidative stress and inflammation in ICR mice. *Neurotoxicology.* 86, 1–9. <https://doi.org/10.1016/j.neuro.2021.06.003>.
- Gustin, K., Tofail, F., Vahter, M., et al, 2018. Cadmium exposure and cognitive abilities and behavior at 10 years of age: a prospective cohort study. *Environ. Int.* 113, 259–268. <https://doi.org/10.1016/j.envint.2018.02.020>.
- Han, C., Lim, Y.H., Hong, Y.C., 2016. Does cadmium exposure contribute to depressive symptoms in the elderly population? *Occup. Environ. Med.* 73, 269–274. <https://doi.org/10.1136/oemed-2015-102900>.
- Hettinger, J.C., Lee, H., Bu, G., et al, 2018. AMPA-ergic regulation of amyloid- β levels in an Alzheimer's disease mouse model. *Mol. Neurodegener.* 13, 22.
- Huat, T.J., Camats-Perna, J., Newcombe, E.A., et al, 2019. Metal toxicity links to Alzheimer's disease and neuroinflammation. *J Mol Biol.* 431, 1843–1868.
- Jiang, H., Li, J., Wang, L., et al, 2020. Total glucosides of paeony: a review of its phytochemistry, role in autoimmune diseases, and mechanisms of action. *J. Ethnopharmacol.* 258, <https://doi.org/10.1016/j.jep.2020.112913> 112913.
- Jonsson, T., Stefansson, H., Steinberg, S., et al, 2013. Variant of TREM2 associated with the risk of Alzheimer's disease. *N. Engl. J. Med.* 368, 107–116.
- Lee, H.K., Takamiya, K., He, K., et al, 2010. Specific roles of AMPA receptor subunit GluR1 (GluA1) phosphorylation sites in regulating synaptic plasticity in the CA1 region of hippocampus. *J. Neurophysiol.* 103, 479–489.
- Li, X.X., Cai, Z.P., Lang, X.Y., et al, 2021. Coeloglossum viride var. bracteatum extract improves cognitive deficits by restoring BDNF, FGF2 levels and suppressing RIP1/RIP3/MLKL-mediated neuroinflammation in a 5xFAD mouse model of Alzheimer's disease. *J. Funct. Foods.* 85, 104612.
- Li, X.X., Lang, X.Y., Ren, T.T., et al, 2022. Coeloglossum viride var. bracteatum extract attenuates A β -induced toxicity by inhibiting RIP1-driven inflammation and necroptosis. *J. Ethnopharmacol.* 282, <https://doi.org/10.1016/j.jep.2021.114606> 114606.
- Li, X., Lv, Y., Yu, S., et al, 2012. The effect of cadmium on A β levels in APP/PS1 transgenic mice. *Exp. Ther. Med.* 4, 125–130.
- Zhang, L., Wang, H., Abel, G.M., et al, 2020. The effects of gene-environment interactions between Cadmium exposure and apolipoprotein E4 on memory in a mouse model of Alzheimer's disease. *J. Toxicol. Sci.*, 173.
- Lingwood, B.E., Healy, G.N., Sullivan, S.M., et al, 2008. MAP2 provides reliable early assessment of neural injury in the newborn piglet model of birth asphyxia. *J. Neurosci. Methods.* 171, 140–146. <https://doi.org/10.1016/j.jneumeth.2008.02.011>.
- Lüscher, C., Malenka, R.C., 2012. NMDA receptor-dependent long-term potentiation and long-term depression (LTP/LTD). *Cold Spring Harb Perspect Biol.*, 4.
- Magee, J.C., Grienberger, C., 2020. Synaptic plasticity forms and functions. *Annu. Rev. Neurosci.* 43, 95–117. <https://doi.org/10.1146/annurev-neuro-090919-022842>.
- Marcondes, L.A., Nachtigall, E.G., Zanluchi, A., et al, 2020. Involvement of medial prefrontal cortex NMDA and AMPA/kainate glutamate receptors in social recognition memory consolidation. *Neurobiol. Learn Mem.* 168, <https://doi.org/10.1016/j.nlm.2019.107153> 107153.
- Min, J.Y., Min, K.B., 2016. Blood cadmium levels and Alzheimer's disease mortality risk in older US adults. *Environ. Health.* 15, 69.
- Minett, T., Classey, J., Matthews, F.E., et al, 2016. Microglial immunophenotype in dementia with Alzheimer's pathology. *J Neuroinflammation* 13, 135.
- Peng, Q., Bakulski, K.M., Nan, B., et al, 2017. Cadmium and Alzheimer's disease mortality in U.S. adults: updated evidence with a urinary biomarker and extended follow-up time. *Environ. Res.* 157, 44–51.
- Qadir, S., Jamshieed, S., Rasool, S., et al, 2014. Modulation of plant growth and metabolism in cadmium-enriched environments. *Rev. Environ. Contam. Toxicol.* 229, 51–88. https://doi.org/10.1007/978-3-319-03777-6_4.
- Qin, S., Hu, X.Y., Xu, H., et al, 2004. Regional alteration of synapsin I in the hippocampal formation of Alzheimer's disease patients. *Acta Neuropathol.* 107, 209–215. <https://doi.org/10.1007/s00401-003-0800-4>.
- Qu, W., Yuan, B., Liu, J., et al, 2021. Emerging role of AMPA receptor subunit GluA1 in synaptic plasticity: implications for Alzheimer's disease. *Cell Prolif.* 54, e12959.
- Reiner, A., Levitz, J., 2018. Glutamatergic signaling in the central nervous system: ionotropic and metabotropic receptors in concert. *Neuron.* 98, 1080–1098. <https://doi.org/10.1016/j.neuron.2018.05.018>.
- Ren, T.T., Yang, J.Y., Wang, J., et al, 2021. Gisenoside Rg1 attenuates cadmium-induced neurotoxicity in vitro and in vivo by attenuating oxidative stress and inflammation. *Inflamm. Res.* 70, 1151–1164. <https://doi.org/10.1007/s00011-021-01513-7>.
- Shu, X.M., Hu, Y., Fang, X., et al, 2022. Salidroside alleviates cadmium-induced toxicity in mice by restoring the notch/HES-1 and RIP1-driven inflammatory signaling axis. *Inflamm Res.* 71, 615–626. <https://doi.org/10.1007/s00011-022-01580-4>.

- Skaper, S.D., Facci, L., Zusso, M., et al, 2017. Synaptic plasticity, dementia and Alzheimer disease. *CNS Neurol. Disord. Drug Targets.* 16, 220–233. <https://doi.org/10.2174/1871527316666170113120853>.
- Steinberg, J.P., Takamiya, K., Shen, Y., et al, 2006. Targeted in vivo mutations of the AMPA receptor subunit GluR2 and its interacting protein PICK1 eliminate cerebellar long-term depression. *Neuron* 49, 845–860. <https://doi.org/10.1016/j.neuron.2006.02.025>.
- Sweatt, J.D., 2001. The neuronal MAP kinase cascade: a biochemical signal integration system subserving synaptic plasticity and memory. *J. Neurochem.* 76, 1–10. <https://doi.org/10.1046/j.1471-4159.2001.00054.x>.
- Tajiri, N., Kellogg, S.L., Shimizu, T., et al, 2013. Traumatic brain injury precipitates cognitive impairment and extracellular A β aggregation in Alzheimer's disease transgenic mice. *PLoS One.* 8, e78851.
- Tu, J., Guo, Y., Hong, W., et al, 2019. The regulatory effects of Paeoniflorin and its derivative Paeoniflorin-6'-O-Benzene Sulfonate CP-25 on inflammation and immune diseases. *Front. Pharmacol.* 10, 57. <https://doi.org/10.3389/fphar.2019.00057>.
- Valois, A.A., Webster, W.S., 1989. The choroid plexus as a target site for cadmium toxicity following chronic exposure in the adult mouse: an ultrastructural study. *Toxicology* 55, 193–205. [https://doi.org/10.1016/0300-483x\(89\)90186-8](https://doi.org/10.1016/0300-483x(89)90186-8).
- Wang, Y.Y., Huang, Z.T., Yuan, M.H., et al, 2021. Role of hypoxia inducible factor-1alpha in Alzheimer's disease. *J. Alzheimers Dis.* 80, 949–961. <https://doi.org/10.3233/JAD-201448>.
- Wendeln, A.C., Degenhardt, K., Kaurani, L., et al, 2018. Innate immune memory in the brain shapes neurological disease hallmarks. *Nature* 556, 332–338. <https://doi.org/10.1038/s41586-018-0023-4>.
- Wilkins, H.M., Carl, S.M., Weber, S.G., et al, 2015. Mitochondrial lysates induce inflammation and Alzheimer's disease-relevant changes in microglial and neuronal cells. *J. Alzheimers Dis.* 45, 305–318.
- Wu, H.T., Yu, Y., Li, X.X., et al, 2021. Edaravone attenuates H₂O₂ or glutamate-induced toxicity in hippocampal neurons and improves AICl₃/D-galactose induced cognitive impairment in mice. *Neurotoxicology* 85, 68–78. <https://doi.org/10.1016/j.neuro.2021.05.005>.
- Yan, H.C., Cao, X., Das, M., et al, 2010. Behavioral animal models of depression. *Neurosci. Bull.* 26, 327–337. <https://doi.org/10.1007/s12264-010-0323-7>.
- Yu, Y., Lang, X.Y., Li, X.X., et al, 2019. 2,3,5,4'-Tetrahydroxystilbene-2-O-beta-d-glucoside attenuates MPP+ /MPTP-induced neurotoxicity in vitro and in vivo by restoring the BDNF-TrkB and FGF2-Akt signaling axis and inhibition of apoptosis. *Food Funct.* 10, 6009–6019. <https://doi.org/10.1039/c9fo01309a>.
- Yuan, Y., Jiang, C.Y., Xu, H., et al, 2013. Cadmium-induced apoptosis in primary rat cerebral cortical neurons culture is mediated by a calcium signaling pathway. *PLoS One* 8, e64330.
- Zhang, S., Hao, S., Qiu, Z., et al, 2019. Cadmium disrupts the DNA damage response by destabilizing RNF168. *Food Chem Toxicol.* 133. <https://doi.org/10.1016/j.fct.2019.110745> 110745.
- Zhong, S.J., Wang, L., Wu, H.T., et al, 2019. *Coeloglossum viride* var. *bracteatum* extract improves learning and memory of chemically-induced aging mice through upregulating neurotrophins BDNF and FGF2 and sequestering neuroinflammation. *J. Funct. Foods.* 57, 40–47.